

ARTICLE

DOI: 10.1038/s41467-018-04812-

OPE

Inducing Kondo screening of vacancy magnetic moments in graphene with gating and local curvature

Yuhang Jiang¹, Po-Wei Lo^{2,3,7}, Daniel May⁴, Guohong Li¹, Guang-Yu Guo^{2,3}, Frithjof B. Anders⁴, Takashi Taniguchi⁵, Kenji Watanabe⁵, Jinhai Mao^{1,6} & Eva Y. Andrei¹

In normal metals the magnetic moment of impurity-spins disappears below a characteristic Kondo temperature which marks the formation of a cloud of conduction-band electrons that screen the local-moment, In contrast, moments embedded in insulators remain unscreened at all temperatures. What then is the fate of magnetic-moments in intermediate, pseudogap systems, such as graphene? Theory predicts that coupling to the conduction-band electrons will drive a quantum phase transition between a local-moment phase and a kondo-screened phase. However, attempts to experimentally confirm this prediction and its intriguing consequences, such as electrostatically tunable magnetic-moments, have been elusive. Here we report the observation of Kondo-screening and the quantum phase-transition between screened and unscreened phases of vacancy magnetic moments in graphene. Using scanning tunneling spectroscopy and numerical renormalization-group calculations we show that this transition enables to control the screening of local moments by tuning the gate voltage and the local curvature of the graphene membrane.

¹Department of Physics and Astronomy, Rutgers University, 136 Frelinghuysen Road, Piscataway, NJ 08855, USA, ² Department of Physics, National Taiwan University, Taipei 10617, Taiwan, ³ Physics Division, National Center for Theoretical Sciences, Hsinchi, 30013, Taiwan, ⁴ Theoretische Physik 2, Technische Universität Dortmand, 44221 Dortmund, Germany, ⁵ Wahnned Materials Laboratory, National Institute for Materials Science, 114 Stankin, Susiuha 305-9044, Japan, ⁶ Institute of Physics, 54 University of Chinese Academy of Sciences, Chinese Academy of Sciences, Beijing 100190, China, ⁷Present address: Department of Physics, Comell University, Hana, NY 14853, USA, Correspondence and requests for materials should be addressed to J.M. (email: jhman@ucas.edu.cn) or to EV.A. (email: andrei@physics.rutgers.edu)

NATURE COMMUNICATIONS | (2018)9:2349 | DOI: 10.1038/s41467-018-04812-6 | www.nature.com/naturecommunication

Graphene, with its linear density of states (DOS) and tunable chemical potential. Provides a playground for exploring the physics of the magnetic quantum phase transition. Grig (Fig. 1a). But embedding a magnetic moment and producing sufficiently large coupling with the itinerant electrons in graphene, poses significant experimental challenges: adatoms typically reside far above the graphene plane, while substitutional atoms tend to become delocalized and non-magnetic. On An alternative and efficient way to embed a magnetic moment in graphene is to create single atom vacancies. The removal of a carbon atom from the honeycomb lattice induces a magnetic moment stemming from the unpaired electrons at the vacancy site. 1-48. This moment has two contributions: one is a resonant state (zero mode-ZM) at the Dirac point (DP) due to the unpaired electron left by the removal of an electron from the raband; the other arises from the broken e-orbitals, two of which hybridize leaving a dangling bond that hosts an unpaired electron. The CM couples ferromagnetically to the dangling o-orbital⁴, as well as to the conduction electrons. And remains unscreened. In flat graphene the magnetic moment from the dangling o-bond is similarly unscreened because the o-orbital is orthogonal to the r-band conduction electrons. Suff. However, it has been proposed that this constraint would be eliminated in the presence of a local curvature which removes the orthogonality of the o-orbital with the conduction had, and enables Kondo screening (6.184). One strategy to introduce local curvature is to deposit the flexible graphene membrane on a corrugated substrate.

Crucially, variations in the local curvature imposed by the cor-Crucally, variations in the local curvature imposed by the cor-rugated substrate provide a range of coupling strengths, from subcritical to the supercritical regime, all in the same sample. An unexpected consequence of this unusually wide variation of coupling strengths is that global measurements such as magne-tization. The resistivity 22 can give contradictory results. In fact, as we will show, the quantum critical transition between Kondo screened and local moment phases in this system, can only be observed through a local measurement.

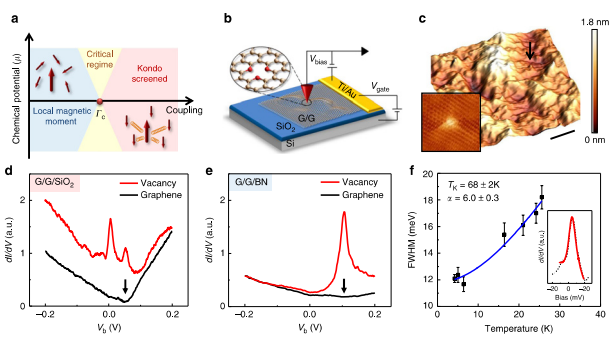


Fig. 1 Kondo peak at a single-atom vacancy in graphene, a Schematic phase diagram of the pseudo-gap Kondo effect. The critical regime (yellow) separates the local-magnetic-moment phase from the Kondo-screened phase. Arrows represent the ground state of the system with the large arrows corresponding to the local spin and the smaller ones representing the spins of electron band. B Schematics of the experiments estimate steps. ESTM topography of a double layer graphene on SIO; (S/G/SIO2). The arrow indicates an isolated vacancy (V_N = 300mV, I= 20pA, V_g = 50 V). The scale bar is 20 nm. Insect atomic resolution topography of a single atom vacancy shows the distinctive triangular structure (4 nm x 4 nm.), Very C200MV, I= 20pA, V_g = 70 V). The row will be structure of the vacancy (lower black curve). The curves are vertically displaced for clarity (V_n = -200MV, I= 20pA, V_g = 0 V). The arrow individes the single structure will be sufficiently displaced for clarity (V_n = -200MV, I= 20pA, V_g = 0 V). The arrow will be structure to the vacancy (lower black curve). The curves are vertically displaced for clarity (V_n = -200MV, I= 20pA, V_g = 0 V). The arrow will be structure the vacancy (lower black curve). The curves are vertically displaced for clarity (V_n = -200MV, I= 20pA, V_g = 0 V). The arrow labels the Dirac prior, the Same as did not avacancy in a G/G/SPN sample (V_p = -200MV, I= 20pA, V_g = -30V), £ Evolution of the measured full width at half maximum (EVHAM) of the Knodo peak with the representable linewidths uncertainty obtained from fitting the Knodo peak to a Fano lineshape. Inset: Zoom into the Knodo peak (black dotted line) together with the Fano lineshape. Etc red solid line)

NATURE COMMUNICATIONS | (2018)9:2349 | DOI: 10.1038/s41467-018-04812-6 | www.nature.com/naturecommunications

zoom in to obtain atomic resolution topography and spectroscopy. Single preparancies are recognized by their distinctive triangular $^{-3}$ Lili 3 R30⁻³ Coopgraphic finge-print (Fig. ic inset) 2^{x-2} 0 which is accompanied by a pronounced peak in the dHdV spectra at the DP reflecting the presence of the ZM. If both the spectra at the DP reflecting the presence of the ZM. If both the see features are present we identify the vacancy as a single atom vacancy (Supplementary Note 2) and proceed to study if further. In order to separate the physics at the DP and the Kondo screening which produces a peak near Fermi energy, F_{x} 1800, the spectrum of the vacancy in Fig. 1d is taken at finite doping corresponding to a chemical potential, $\frac{100}{2}F_{x}-F_{D}=-5^{2}$ meV. For from the vacancy (lower curve), we observe the V shaped spectrum characteristic of pristine graphene, with the minimum identifying the DP energy. In contrast, at the center of the vacancy (Fig. 1d upper curve), the spectrum features two peaks, one at the DP identifying the ZM and the other at zero bias coincides with the position of the expected Kondo peak' (In SISS the zero-bias is identified with $F_{x,y}$). From the line shape of the zero-bias is identified with $F_{x,y}$) From the line shape of the zero-bias peak (Fig. 1 finset), we extract $T_{x,y} = (67\pm2)K$ by fitting the Fig. 1 finset), we extract $T_{x,y} = (67\pm2)K$ by fitting the Fig. 1 finset), we extract $T_{x,y} = (67\pm2)K$ (Supplementary Note 3). As a further independent check we compare in Fig. 1 the temperature dependence of the linewidth to that expected for a Kentural property of the property of

Numerical renormalization group calculations. To better understand the experimental results we performed numerical renormalization-group (NRG) calculations for a minimal model based on the pseudogap asymmetric Anderson impurity model (AIM).6-16.5 comprising the free local α -orbital coupled to the itinerant π -band (Supplementary Note 6). This model gives an accurate description of the experiment in the p-doped regime where the ZM is sufficiently far from the Kondo peak so that their overlap is needligible. Upon approaching charge neutrality, intervende is needligible. where the ZM is suthiciently far from the Kondo peak so that their overlap is negligible. Upon approaching charge neutrality, interactions between the two orbitals through Hund's coupling and level repulsion become relevant. As described in Supplementary Note 6 we introduced an effective Coulomb interaction term to take into account this additional repulsion. The single orbital model together with this phenomenological correction captures the main features of the Kondo physics reported here (Fig. 3).

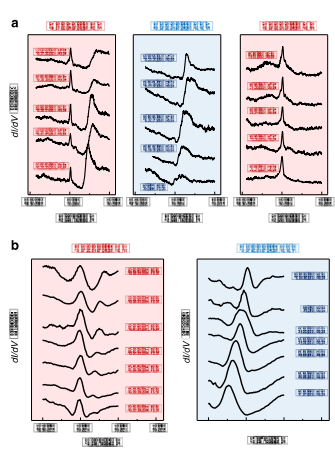


Fig. 2 Evolution of Kondo screening with chemical potential, a dl/dV curves for a subcritical Kondo vacancy (type I in text) with reduced coupling strength $\mathbb{R}/(\mathbb{R}) = 0.90$ at the indicated values of chemical potential, Red (blue) shade indicates the presence (absence) of the Kondo peak $(V_b = -200\text{mV}, J = 20\text{pA})$. The chemical potential is tuned by the backgate voltages? b, d/dV curves for a supercritical Kondo vacancy (type II in text) with $\mathbb{R}/\mathbb{R} = 1.83$

Results from a comprehensive NRG calculation using a two-orbital pseudogap AlM to model the problem signifiarly indicate that this simplified one-orbital approach qualitatively describes the experimental results. The single orbital AlM is characterized by three energy scales. [\$\frac{1}{3}\$ U, and \$\frac{1}{3}\$ corresponding to the energy of the impurity state, the onsite Coulomb repulsion, and by the scattering rate or exchange between the impurity and the con-duction electrons, respectively (Supplementary Note 7). In the asymmetric AlM, which is relevant to screening of vacancy magnetic moments in granbene, the particle-hole symmetry is asymmetric AIM, which is relevant to screening of vacancy magnetic moments in graphene, the particle-hole symmetry is broken by next-nearest neighbor hopping and by University broken by next-nearest neighbor hopping and by University broken by next-nearest neighbor hopping and by University broken by RG phase diagram for this model is controlled by the valence fluctuation (VF) critical point, [1] 10 phase parameters the NRG flow into two soctors supercritical. [2] 20 which flows to the asymmetric strong-coupling (ASC) fixed which flows to the asymmetric strong-coupling (ASC) fixed > \(\begin{align*} \) which flows to the asymmetric strong-coupling (ASC) fixed point where charge fluctuations give rise to a frozen impurity (FI) ground state \(\begin{align*} \), and subcritical. \(\begin{align*} \begin{align*} \begin{align*} \begin{align*} \) which flows to the local moment (LM) fixed point where the impurity moment is unscreened. At the FI fixed point, the correlated ground state acquires one additional charge due to the enhancement of the particle-hole asymmetry in the RG flow. In a simplified picture, the fixed point spectrum can be understood by the flow of \(\begin{align*} \begin{alig

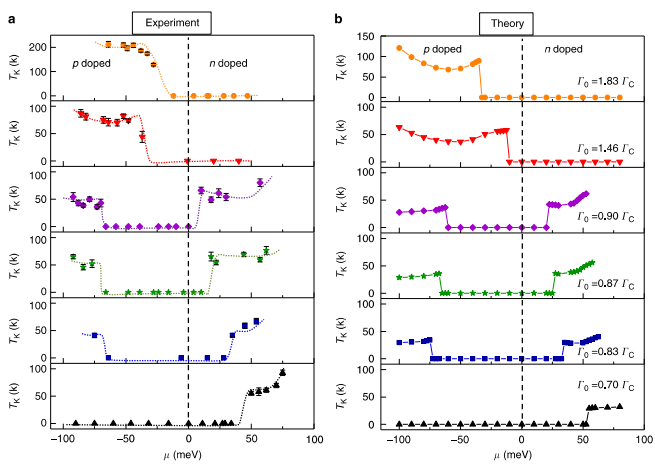


Fig. 3 Chemical-potential dependence of the Kon peak. In the regions where the peak is absent we simulated Kondo peak (Supplementary Note 3) be of the Kondo temperature, a Chemical potential dependence of T_K obtained from the Fano lineshape fit of the Kondo is absent we designated $T_K = 0$. b NRG result for the vacancies in panel a, T_K is estimated by fitting the numerically

conduction band and the local orbital with a small enhancement of $n_0 = 1.2 - 1.3$. For $[] \mathbb{Z} \setminus []$ and $[] \mathbb{Z}]$ by the appearance of relevant spin fluctuations gives rise to a cloud of spin-polarized electrons that screen the local moment below a characteristic temperature T_K which is exponentially suppressed (10.7) $[] \mathbb{Z}] \mathbb{Z}] \mathbb{Z}] \mathbb{Z} \mathbb{Z}$ a result, at sufficiently low doping, T_K must fall below any experimentally accessible temperature, so that for all practical purposes its value can be set to zero $(F \|_{2}, 4)$. Using NRC to simulate the experimental spectra (Supplementary Note $2 \times V^{1-2\omega d}$ and a critical coupling $[\mathbb{Z}] = 1.5 \times V^{1-2\omega d}$ and a flast obtained the value of the reduced coupling $[\mathbb{Z}] = 1.5 \times V^{1-2\omega d}$ and a flast obtained the value of the reduced coupling $[\mathbb{Z}] = 1.5 \times V^{1-2\omega d}$ and a flast obtained for the spectra in Fig. 2a, by place these two vacancies in the sub-critical and super-critical regimes respectively.

In Fig. 3 we compare the chemical-potential dependence of the measured T_K , with the NRG results. The T_K values are obtained from Fano-fits of the Kondo peaks leading to the T_K $[\mathbb{Z}]$ curves obtained by using NRG to simulate the spectra are shown in Fig. 3b. The close agreement between experiment and simulations confirms the validity of the asymmetric AIM for elsewing T_K T_K T

finite doping ($\mathbb{H}\mathbb{H}0$) and is marked by the appearance of the Kondo-peak.^{8,9} The phase diagram clearly shows the strong electron-hole asymmetry consistent with the asymmetric screening expected in in this system.⁴

Dependence of Kondo screening on corrugation amplitude. Theoretical work!6.44 suggests that coupling of the vacancy moment with the conduction electrons in graphene may occur if local corrugations produce an out of plane component of the dangling σ-orbital. This removes the orthogonality restriction of that prevents hybridization of the σ-bands and π-bands in that graphene and produces a finite coupling strength which increases monotonically with the out of plane projection of the orbital 18.19.45. To check this conjecture we repeated the experiments for samples on substrates with different average corrugation amplitudes as shown in Fig. 9 ds. c. For consistency all the fabrication steps were identical. In the G/SiO₂ sample (single layer graphene on SiO₂) where the corrugation amplitude was largest (~1 nm), 60% of the vacancies displayed the Kondo peak and T_k statianed values as high as 180 K (Supplementary Note 5). For the flatter G/G/SiO₂ where the average corrugation was ~0.5 nm, we found that 30% of the vacancies showed the Kondo peak with T_k values up to 70 K. For samples deposited on hBN, which were the lattest with local corrugation amplitudes of ~0.1 nm, none of the vacancies showed the Kondo peak. This is illustrated in Fig. 1e showing a typical dIIIdV curve on a vacancy in G/G/BN (double layer graphene on hBN) where a gate voltage of V_g = ~30V was applied to separate the energies of E_g and the DP. While this 10338/484169-0208-048126 [www.adulue.com/naturecommunications

NATURE COMMUNICATIONS I (2018)9:2349 I DOI: 10.1038/s41467-018-04812-6 I www.nature.com/naturecomm

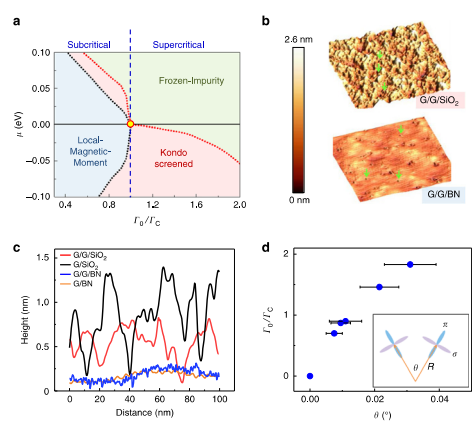


Fig. 4 Quantum phase transition and Kondo screening. a [IIII] phase diagram at 4.2 K. The critical coupling [III] (circle at [III]/III] = 1.0) designates the boundary between frozen-impurity and the Local-Magnetic-Moment phases at [III] 0. Dotted lines represent boundaries between the phases (Supplementary Note 3). B STM topography for the GyG/SIO, (topo) and GyG/SIO, (toto) and samples with the same scale bat (V. 200MX). The arrows point to the vacancies. C Typical line profile of the STM topographies of graphene on different substrates with the same scanning parameters as in b. d The evolution of the hybridization strength with the curvature. Error bars represent the uncertainty in obtaining the angle between the [III] and the local graphene plane orientation from the local topography measurements, Inset: sketch of the curvature effect on the orbital hybridization

spectrum shows a clear ZM peak, the Kondo peak is absent over the entire range of doping. The absence of the Kondo peak is all the samples deposited on hBN highlights the importance of the local curvature. In order to quantify the effect of the local curvature on the coupling strength, we employed STM topography to measure the local radius of curvature, R. at the vacancy sites (Fig. 4d inset) from which we estimate the angle between the orbital and the local graphene plane orientation. Statistics (Fig. 4d), consistent with the coupling strength, the decrease of the curvature of the Kondo coupling was also observed for Co atoms deposited on corrugated graphene. And was also utilized to enhance the spin-orbit coupling.

Discussion

DiscussionThe results presented here shed light on the contradictory conclusions drawn from earlier magnetometry ^{50,21} and transport measurements²² on irradiation induced vacancies in graphene. While the transport measurements revealed a resistivity minimum and logarithmic scaling indicative of Kondo screening with nunsually large values of T_F ~ 90 K, magnetometry measurements showed Curie behavior with no evidence of low-temperature saturation, suggesting that the vacancy moments remained unscreened. To understand the origin of this discrepancy we note that magnetometry and transport are sensitive to complementary aspects of the Kondo effect. The former probes the magnetic moment and therefore only sees vacancies that are not screened,

while the latter probes the enhanced scattering from the Kondo cloud which selects only the vacancies whose moment is Kondo screened. Importantly, these techniques take a global average over all the vacancies in the sample. This does not pose a problem when all the impurities have identical coupling strengths. But if there is a distribution of couplings ranging from zero to finite values, as is the case here, global magnetization and transport measurements will necessarily lead to opposite conclusions as reported in the earlier work.

measurements will necessarily lead to opposite conclusions as reported in the earlier work.

The local spectroscopy technique employed here made it possible to disentangle the physics of Kondo screening in the presence of a distribution of coupling strengths. This work demonstrates the existence of Kondo screening in a pseudogap system and identifies the quantum phase transition between a screened and an unscreened local magnetic moment. It further shows that the local magnetic moment can be tuned both electrically and mechanically, by using a gate voltage and a local curvature, respectively. curvature, respectively.

Mothods

Sample fabrication. The GiG/SiO₂ samples consisted of two stacked graphene layers deposited on a 300 nm SiO₂ dielectric layer capping a highly doped Si chip (acting as the backgate electrods)^{23,66,67}. The bottom graphene layer was setfoliated to the SiO₂ surface and the second layer was stacked on top by a dy transfer process. PMMA and PVA thin films were used as the carrier in the dry transfer process. Auril electrodes were aduled by standard SiA lithography, followed process. Auril electrodes were aduled by standard SiA lithography, followed graphs and the process. Auril electrodes were aduled by standard SiA lithography, followed graphs and six process. Auril electrodes were aduled by standard SiA lithography, followed graphs and six process. The process of the process o

introduce single vacancies in the graphene lattice, the device was exposed under UHV conditions to a beam of $\mathrm{He^+}$ ions with energy $100\,\mathrm{eV}$ for 5 to $10\,\mathrm{s}$, and further amended at high temperature in single⁸.

Scanning tunneling microscopy experiment. Except where mentioned all the STM experiments were performed at 42.K. dildV curves were collected by the standard lock-in technique, with 0.5 mW AC modulation at 473 Hz added to the DC sample bias^{2-6,50}. The chemical potential was tuned by the backgate voltage as illustrated in Fig. 1b.

Received: 1 February 2018 Accepted: 10 May 2018 Published online: 14 June 2018

References

- Castro Neto, A. H., Guinea, F., Peres, N. M. R., Novoselov, K. S. & Geim, A. K. The electronic properties of graphene. *Rev. Mod. Phys.* 81, 109–162
- (2009).
 Andrel, E. V., Li, G. H. R. Diu, X. Betronic properties of graphene a perspective from scanning tumeling microscopy and magnetotramport. Rep. Prog. Phys. 75, 65607 (2012).
 Hewson, A. C. The Kondo Problem to Heavy Fermions (Cambridge University Press, Cambridge, 1997).
 Withoff, D. & Fradkin, E. Phase transitions in gapless fermi systems with magnetic impurities. Phys. Rev. Lett. 64, 1833–1838 (1998).
 Cassanello, C. R. & Fradkin, E. Kondo effect in flux phases. Phys. Rev. B 53, 15079–13098 (1996).

- 15079—15094 (1996).
 Gonzalez-Busto, C. & Ingersent, K. Renormalization-group study of Anderson and Kondo impurities in gapless Fermi systems. Phys. Rev. B 57, 14251–1429 (1997).
 Fritz, L. & Voja, M. Phase transitions in the pseudogap Anderson and Kondo models: critical dimensions, renormalization group, and local-moment criticality. Phys. Rev. B 70, 214427 (2004).
 Voya, M., Fritz, L. & Bolla, R. Gatte-ortholdel Kondo screening in graphene: quantum criticality and electron-hole asymmetry. Europhys. Lett. 90, 27006 (2010). (2010).

- (2010).

 Quality S. Kanson, T. Matsuurs, H. & Ogata, M. Theory of defect-induced kondo effect in graphene: numerical enormalization group study, J. Phys. Soc. Jpn 81, 063709 (2012).

 Quality S. G. Margher, G. Margher, G. Margher, G. Margher, G. Margher, C. Margher, G. M

- Li, G., Luican, A. & Andrei, E. Y. Self-navigation of a scanning tunneling microscope tip toward a micron-sized graphene sample. Rev. Sci. Instrum. 82, 073701 (2011).

- mcrocope tip loward a micron sized graphene sample. Rev. Xr. Instrum. 82, 073701 (2011).

 Or Storic (2011). In Diversities of Van Bree singularities in twisted graphene layers. Nat. Phys. 6, 109–113 (2010).

 Luican, A. et al. Single-layer behavior and its breakdown in twisted graphene layers. Phys. Rev. Lett. 106, 128002 (2011).

 Ugada, M. N., Bribuga, I., Culmen, F. & Gomer-Rodriguez, J. M. Missing atom as a source of carbon magnetism. Phys. Rev. Lett. 104, 096804 (2010).

 S. Mao, J. et al. Realization of a tunable artificial atom at a charged venarious of the phys. Rev. Lett. 104, 096804 (2010).

 S. Mai, P. et al. Realization of a tunable artificial atom at a charged venarious consistence of the physical control of the Kondo effect on single adatoms. J. Phys. Condens. Matter 21, 053001 (2000).

- ed: I February 2018 Accepted: 10 May 2018 and online: 14 June 2018

 Increas. M. Feinstein, A. E. Schiender, W. D. Spectroscopic manifestations of Committee and Committee

Acknowledgements

Acknowledgements

We acknowledge support from DOE-FG02-99ER45742 (EY.A. and J.M.), NSF DMR
1788158 (Y.J.), Ministry of Science and Technology and also Academia Sinica of Taislum,
(G.Y.G. and PW.L.), Deutsche Forschungsgemeinschaft by project AN2757851,
and F.B.A.), Key Research Program of the Chinese Academy of Sciences XDPB08-1

(G.M.), We than Natura Andrie, Brome Udosa and Mobiama Sherafald for useful (J.M.), We than Natura Andrie, Brome Udosa and Mobiama Sherafald for useful (J.M.), We than Natura Andrie, Brome Udosa and Mobiama Sherafald for useful (J.M.), We than Natura Andrie, Brome Udosa and Mobiama Sherafald for useful (J.M.), We than Natura Andrie, Brome Udosa and Mobiama Sherafald for useful (J.M.), We than Natura Andrie, Brome Udosa and Mobiama Sherafald for useful (J.M.), We than Natura Andrie Rome Udosa and Mobiama Sherafald for useful (J.M.).

Author contributions
Y.J., JM., and E.Y.A. concrived the work and designed the research strategy, Y.J. and J.
performed the experiments, analyzed data, and wrote the paper, G.L. built the STM.
P.W.L., D.M., G.Y.G., and F.B.A. carried out the theoretical work. T.T. and K.W.

Publisher's note: Springer Nature remains neutral with regard to jurisdictional claims in published maps and institutional affiliations.

⊗ The Author(s) 2018

Contributed the boron nitride EVA. directed the project, analyzed the data, and wrote the paper.

Additional information
Supplementary Information companies this paper at https://doi.org/10.1038/s41467018-01812-6.

Competing interests: The authors declare no competing interests.

Reprints and permission information is available online at http://mpg.nature.com/
reprintsand/permissions/